ACS APPLIED MATERIALS & INTERFACES

Research Article

Cite This: ACS Appl. Mater. Interfaces 2018, 10, 9444−9450

www.acsami.org

Highly Ordered Hierarchical Pt and PtNi Nanowire Arrays for Enhanced Electrocatalytic Activity toward Methanol Oxidation

Changzheng Wang,[†] Yang Zhang,[*,‡] Yajun Zhang,[†] Ping Xu,[†] Cuimin Feng,[†] Tao Chen,[†] Tao Guo,[†] Fengnan Yang,[†] Qiang Wang,[*,§] Jingxiao Wang,[†] Mengtong Shi,[†] Louzhen Fan,[*,∥] and Shaowei Chen[*,⊥]

[†]Key Laboratory of Urban Stormwater System and Water Environment, Ministry of Education, Beijing University of Civil Engineering and Architecture, Beijing 100044, China

[‡]Beijing Institute of Nanoenergy and Nanosystems, Chinese Academy of Sciences, Beijing 100083, China

[§]Laboratory for Micro-sized Functional Materials, College of Elementary Education, Capital Normal University, Beijing 100048, China

[∥]Department of Chemistry, Beijing Normal University, Beijing 100875, China

[⊥]Department of Chemistry and Biochemistry, University of California, Santa Cruz, California 95064, United States

Supporting Information

ABSTRACT: Highly ordered hierarchical Pt and PtNi nanowire arrays were prepared using CdS hierarchical nanowire arrays (HNWAs) as sacrificial templates and demonstrated high electrochemical active surface areas. For the resulting Pt HNWAs sample, the peak current for methanol oxidation at +0.74 V was almost 1 order of magnitude higher than that of Pt solid nanowire arrays prepared in a similar manner but without the use of CdS template, and the addition of a Ni cocatalyst effectively enhanced the tolerance against CO poisoning. The results demonstrated that highly ordered Pt and PtNi HNWAs may be exploited as promising anode catalysts in the application of direct methanol fuel cells.

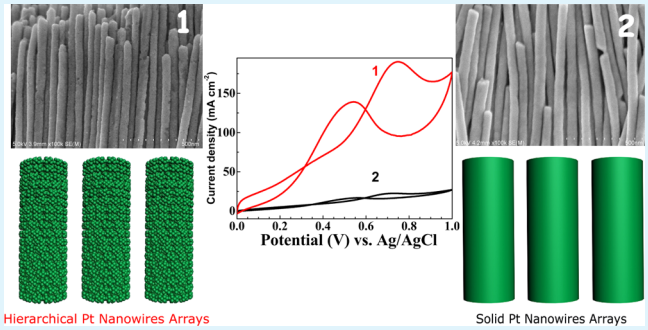

KEYWORDS: *nanowire arrays, hierarchical nanostructure, methanol oxidation reaction, DMFCs, CdS nanoparticles*

1. INTRODUCTION

Direct methanol fuel cells (DMFCs) have gained extensive attention as a promising technology in powering portable electronic devices due to the high energy density of methanol, low operating temperature, the abundance of methanol, and ease of handling liquid fuels.[1−7] Pt-based nanomaterials have been used extensively as the anode catalysts for methanol oxidation.[8] However, the widespread applications of DMFCs have been hampered by the low natural abundance, high costs, and susceptibility to poisoning of Pt.[9] Thus, substantial efforts have been devoted to the structural engineering of nanostructured Pt catalysts, in particular, with regard to composition, morphology, and dimension, so as to improve the utilization efficiency of Pt and enhance the electrocatalytic performance.[10−12] Toward this end, one effective approach is to synthesize Pt-based catalysts with high surface areas and surface-to-volume ratios.[13−16] In fact, in recent studies, a wide range of Pt-based nanostructures have been produced, including spherical particles, nanoclusters, nanorods/wires, star-shaped particles, branched multipods, dendritic nanogarlands, etc.,[17−28] and dispersed on appropriate supporting materials.[29−33] For instance, Pt-nanoparticle (NP) catalysts have been deposited on carbon nanotubes, carbon fibers, fullerene, graphene, and nanoporous graphitic carbon materials,[8,16,21,28,34−37] and the use of these lightweight, high-surface-area catalyst supports leads to good dispersion of the Pt NPs, which facilitates surface accessibility and electron-transfer kinetics. The effective electrochemical surface areas may also be enhanced by the formation of hierarchical platinum nanostructures. For instance, ordered nanowire arrays have been readily prepared by utilizing anodic aluminum oxide (AAO) template with tunable pore diameter and channel length, and mesoporous Pt fibers have been prepared by photoreduction or electrochemical reduction of metal precursors dissolved in the aqueous solution.[38,39] The formation of a large number of edge and corner Pt atoms plays an essential role in enhancing the electrocatalytic activity toward methanol oxidation.

Received: December 28, 2017
Accepted: February 23, 2018
Published: February 23, 2018

DOI: 10.1021/acsami.7b19727
ACS Appl. Mater. Interfaces 2018, 10, 9444−9450

In addition, it has been demonstrated that in contrast to monometallic Pt catalysts, which are prone to poisoning during methanol oxidation reaction, alloying of Pt with a second transition metal significantly can enhance the resistance against poisoning species.[40−47] For instance, marked enhancement has been observed with Pt−Ru and Pt−Pd alloys, and cocatalysts, such as Ni, Cu, Mo and Co, actually have also been used due to their high abundances and low costs.[46−52] The formation of such Pt−M alloy structures leads to weakened Pt−CO binding interactions and the formation of OH species at a reduced potential that is reactive with intermediates on the catalyst surfaces.[53−55] That is, the incorporation of cocatalysts reduces the loading of expensive Pt, enhances resistance against poisoning, improves catalyst stability and durability, and ultimately the overall energy conversion efficiency.

In the present study, Pt and PtNi hierarchical nanowire arrays (HNWAs) were prepared by a facile procedure based on CdS HNWAs templates and used as effective catalysts toward methanol oxidation. The CdS HNWAs were prepared by the deposition of CdS NPs into nanoporous AAO template and then served as a sacrificial template for the preparation of Pt or PtNi HNWAs. The simultaneous dissolution of CdS NPs and electrochemical deposition of Pt (or PtNi) HNWAs in aqueous solution were conducted at ambient temperature. The as-prepared nanostructured Pt and PtNi HNWAs were characterized by a wide range of spectroscopic measurements. Electrochemical measurements showed that in comparison to Pt solid nanowire arrays (SNWAs) that were prepared without the use of CdS HNWAs as sacrificial templates, Pt HNWAs demonstrated remarkably enhanced electrocatalytic activity for methanol oxidation. Further improvement of the electrocatalytic activity was achieved by the preparation of PtNi alloy HNWAs where CO poisoning of the catalysts was considerably reduced.

2. EXPERIMENTAL SECTION

2.1. Chemicals. All reagents in this work, such as sublimed sulfur (S), dimethyl sulfoxide, cadmium acetate ($Cd(CH_3COO)_2$), tetrachloroethylene, octylamine, potassium hexachloroplatinate (K_2PtCl_6), nickel chloride ($NiCl_2$), sulfuric acid (H_2SO_4), and methanol were purchased from Beijing Chemical Works and used as received without further purification. AAO templates were prepared by two-step anodization of aluminum plates in oxalic acid solution.[31] The pore diameter of AAO template was about 60−80 nm.

2.2. Preparation of CdS HNWAs. CdS HNWAs were prepared according to a previous procedure with some modifications.[56] First, one side of AAO template was deposited on a Pt film and then heated in air for 5 min. Second, the AAO template was immersed in a tetrachloroethylene solution containing CdS colloids for 24 h at 20 °C and then an ethanol/tetrachloroethylene mixed solvent (v/v = 1:6) was added dropwise into the CdS colloid solution to induce deposition of CdS NPs into the AAO channels.[31] Finally, excess CdS NPs on the top of the AAO template were removed by polishing.

2.3. Preparation of Pt and PtNi HNWAs and Pt SNWAs. In a three-electrode system, the CdS HNWA-loaded Pt disk prepared above was used as the working electrode, a Pt wire as the counter electrode, and Ag/AgCl as the reference electrode. The working electrode was biased at −0.4 V in a solution containing 1 mM K_2PtCl_6 and 0.1 M H_2SO_4 over different periods of time. PtNi HNWAs were fabricated in a similar fashion in a 0.1 M H_2SO_4 solution containing 1 mM K_2PtCl_6 and 1 mM $NiCl_2$. The Pt and PtNi SNWAs samples were also prepared using the AAO template but without CdS HNWAs as sacrificial templates. The mass of Pt in HNWAs and SNWAs was well controlled by the electric quantity during the electrodeposition process.

2.4. Characterization. The morphology and size of the as-prepared samples were investigated by scanning electron microscopy (SEM, Hitachi S4800) with energy-dispersive X-ray (EDX) and transmission electron microscopy (TEM, JEOL2011 and F20). X-ray diffraction (XRD) measurements were performed on a Shimadzu XRD-6000 using Cu Kα radiation (1.5406 Å) and operated at 40 kV and 20 mA. X-ray photoelectron spectroscopy (XPS) data were obtained with an ESCALab220i-XL electron spectrometer (VG Scientific) using 300 W Mg Kα radiation. The data were referenced to the C 1s line at 284.8 eV from adventitious carbon. Electrochemical experiments were conducted using a CHI 660 analyzer (CH Instruments) with the nanowire arrays prepared above as the working electrode, Ag/AgCl as the reference electrode, and a platinum wire as the counter electrode. The measurements were conducted at 20 °C. For each measurement, the geometric area of the working electrode was fixed to be 1 cm^2.

3. RESULTS AND DISCUSSION

The preparation of Pt HNWAs is schematically depicted in Figure 1. The AAO template with CdS HNWAs was immersed

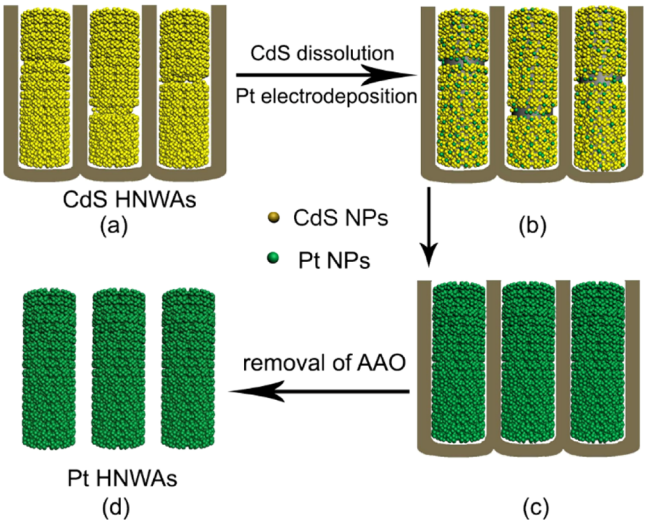

Figure 1. Schematic illustration of the formation process of Pt HNWAs. (a) Synthesis of CdS HNWAs in AAO template; (b) dissolution of CdS NPs and electrodeposition of Pt NPs; (c) formation of Pt HNWAs in AAO template, and (d) removal of AAO template.

into a K_2PtCl_6/H_2SO_4 solution, leading to dissolution of the CdS NPs and generation of Pt NPs in the void space between adjacent CdS NPs by electrochemical deposition. After the removal of the AAO template, highly ordered Pt (or PtNi) HNWAs were obtained.

The formation of CdS HNWAs was shown in the SEM measurements (Figure S1), which entailed the aggregated assembly of CdS NPs.[56] Part of the CdS HNWAs was broken during sample preparation due to limited mechanical strength. Representative SEM images of Pt HNWAs with a deposition time of 3600 s are presented in Figure 2a−c. It can be seen that after the removal of the AAO template, the Pt HNWAs remained vertically aligned on the substrate surface and the mechanical strength of Pt HNWAs was markedly enhanced compared to that of CdS HNWAs. The diameter of the obtained hierarchically structured Pt nanowires is approximately 50 nm, which is close to the pore size of the original AAO template. The inset to Figure 2c shows a high-magnification SEM side-view image, which further unveils the

DOI: 10.1021/acsami.7b19727
ACS Appl. Mater. Interfaces 2018, 10, 9444−9450

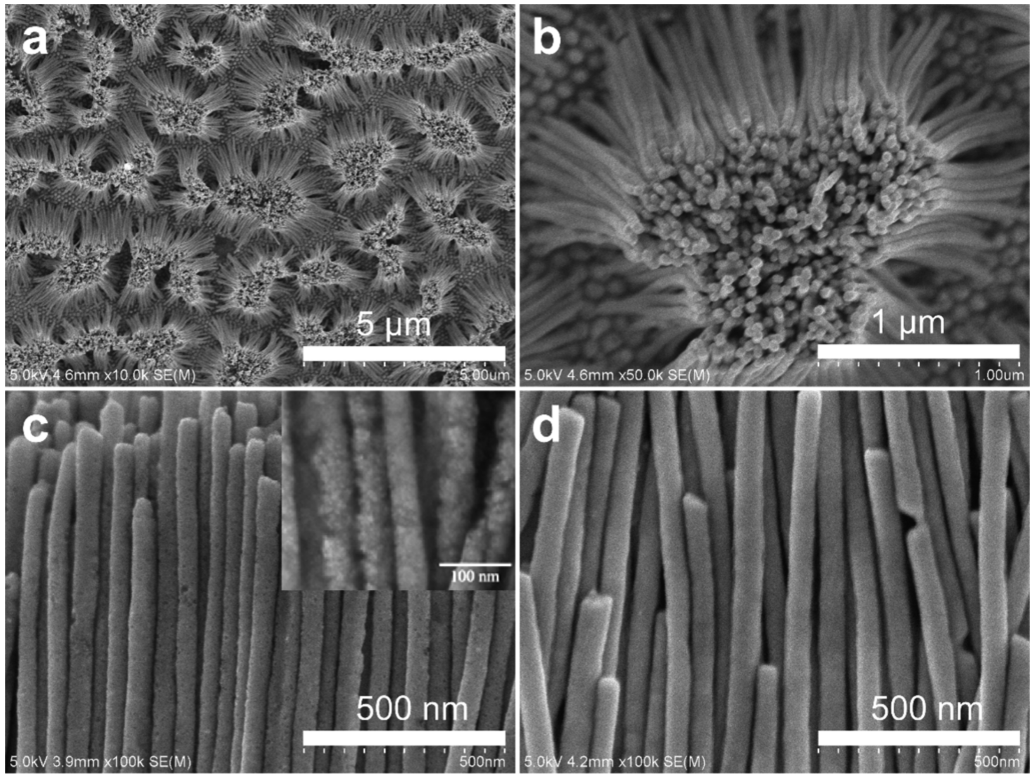

Figure 2. SEM top-view images of Pt HNWAs at (a) low- and (b) high-magnification, side-view image of (c) as-synthesized Pt HNWAs and (d) Pt SNWAs; the inset of (c) shows a higher magnification view.

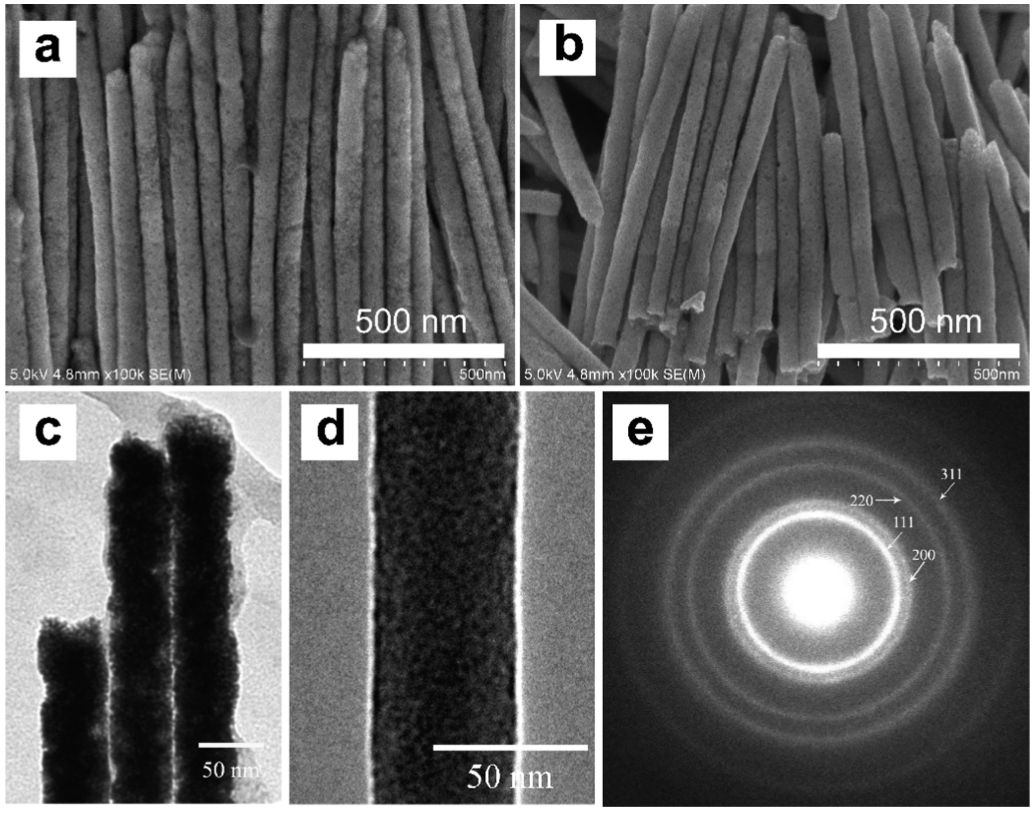

Figure 3. SEM images of Pt HNWAs prepared at different Pt electrodeposition times: (a) 600 s and (b) 7200 s. (c, d) Typical TEM images and (e) SAED patterns of Pt hierarchical nanowires.

distinctive hierarchical characteristics of individual Pt nanowires. For comparison, Pt SNWAs were directly electrodeposited into a CdS-free AAO template and exhibited a markedly different surface morphology as compared to that of

DOI: 10.1021/acsami.7b19727
ACS Appl. Mater. Interfaces 2018, 10, 9444−9450

Pt HNWAs. As demonstrated in Figure 1c,d, Pt HNWAs were built by separated Pt NPs, whereas Pt SNWAs exhibited a smooth surface and no individual NPs could be identified. Therefore, it can be concluded that CdS HNWAs played an indispensable role in synthesizing Pt HNWAs by serving as the sacrificial templates.

Furthermore, the morphology of the Pt HNWAs also varied with the electrodeposition time. From Figure 3a,b, one can see that when the electrodeposition time was increased from 600 to 7200 s, the void space between Pt NPs decreased accordingly. The structures of the Pt HNWAs were further studied by TEM measurements. From Figure 3c,d, it can be clearly observed that the hierarchical nanowires were indeed composed of separated Pt NPs, and the corresponding selected area electron diffraction (SAED) patterns were indicative of polycrystalline nature with well-defined diffraction rings of the (111), (200), (220), and (311) crystalline planes, in good agreement with the face-centered cubic structure of Pt (Figure 3e).[57] The EDX measurements (Figure S2) further confirmed the presence of platinum, cadmium, and sulfur elements due to incomplete dissolution of the CdS scaffold in the formation of hierarchical Pt (or PtNi) HNWAs. Although CdS has no contribution to the electrocatalytic activity toward methanol oxidation, CdS nanowire arrays play an essential role in designing and fabricating efficient Pt-based electrocatalysts. Because of their hierarchical nanoarchitecture, the employment of CdS HNWAs can avoid the aggregation of Pt and exhibit the high catalytic activity of Pt-based electrocatalysts. In comparison with Pt SNWAs, Pt HNWAs can be facilely prepared via a sacrificial template method by simultaneous dissolution of CdS NPs and deposition of Pt NPs. Particularly, as-synthesized CdS NPs with a size of 2−5 nm can be considered as ideal nanoscale building blocks for the hierarchical assembly for the preparation of CdS HNWAs.

The structures of Pt HNWAs were further examined by X-ray spectroscopic measurements. From the XRD patterns in Figure S3, four diffraction peaks can be identified at 2θ = 40, 46, 65, and 78°, which may be assigned to the diffractions of the (111), (200), (220), and (311) crystalline planes, respectively, of face-centered cubic crystal structure Pt.[58,59] In XPS measurements (Figure S4), two bands emerged at 70.9 and 74.1 eV, corresponding to the Pt $4f_{7/2}$ and Pt $4f_{5/2}$ electrons of metallic Pt, respectively.[60−62] Note that the Pt 4f binding energies of Pt HNWAs were somewhat lower than those of Pt SNWAs (70.9 and 74.1 eV), likely due to intimate contact and electronic interactions between the electrodeposited Pt and residual CdS in the former.

The electrocatalytic activity toward methanol oxidation was then examined by electrochemical measurements. Figure S5 depicts the cyclic voltammograms of Pt HNWAs (curve 1) and Pt SNWAs (curve 2) in 0.5 M H_2SO_4, where two pairs of voltammetric peaks can be seen within the potential range of −0.2 to +0.2 V due to the hydrogen adsorption/desorption on the Pt surfaces. In addition, a pair of broad peaks can be seen between +0.2 and +1.0 V, which arose from the redox reactions of platinum oxides. From these butterfly features, the effective electrochemically active surface area (ECSA) was estimated to be 600 cm^2/mg for Pt HNWAs, which was substantially larger than that of Pt SNWAs (140 cm^2/mg).[63] This may be attributed to the unique hierarchical nanostructure of Pt HNWAs. The electrocatalytic activities toward methanol oxidation were then investigated and compared. Figure 4a shows the voltammograms of Pt HNWAs (curve 1) and

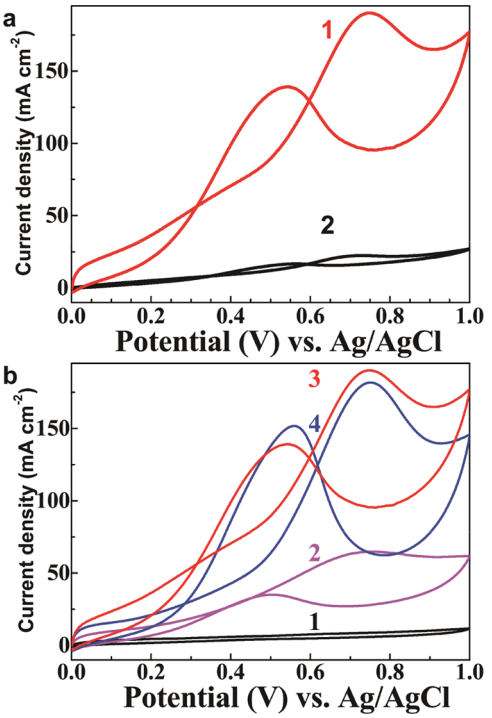

Figure 4. (a) Cyclic voltammograms of (curve 1) Pt HNWAs and (curve 2) Pt SNWAs in a solution containing 0.5 M CH_3OH and 0.5 M H_2SO_4. The potential scan rate is 50 mV/s; (b) cyclic voltammograms of Pt HNWAs in a solution containing 0.5 M CH_3OH and 0.5 M H_2SO_4, Pt HNWAs samples were prepared at different electrodeposition times: (curve 1) 60 s, (curve 2) 600 s, (curve 3) 3600 s, and (curve 4) 7200 s. The potential scan rate is 50 mV/s.

SNWAs (curve 2) in a solution containing 0.5 M H_2SO_4 and 0.5 M CH_3OH at the same mass loading. It can be seen that on both Pt electrodes, a voltammetric peak appeared in the anodic scan at ca. +0.74 V, and in the return scan, an anodic peak can also be found at +0.54 V, signifying the apparent activity of both Pt HNWAs and SNWAs toward methanol oxidation. Yet, one can see that the anodic peak current of Pt HNWAs was almost 1 order of magnitude higher than that of Pt SNWAs. This may be ascribed to the larger ECSA of the former. In Pt HNWAs, both the exterior and interior surfaces of the separated Pt NPs were readily accessible in comparison to that of Pt SNWAs where the compact arrangements reduced the accessible surface area significantly. Furthermore, the electrochemical activity of the Pt HNWAs was found to vary with the electrodeposition time, as depicted in Figure 4b. When the electrodeposition time was increased from 60 to 3600 s, the anodic peak current density of methanol oxidation increased markedly from 65 to 190 mA/cm^2. However, with a further increase of the deposition time to 7200 s, a slight decrease of the voltammetric peak current was observed instead. This may be due to the overloading of Pt NPs that resulted in reduced effective surface area.

Note that in methanol oxidation, Pt has been known to be prone to CO poisoning. To enhance the resistance against CO poisoning and decrease the loading of Pt catalysts, PtNi alloy HNWAs and SNWAs were also prepared in the same manner and the electrocatalytic activities for methanol oxidation were quantified and compared. In comparison with Pt HNWAs, comparable surface morphology was observed with the PtNi

DOI: 10.1021/acsami.7b19727
ACS Appl. Mater. Interfaces 2018, 10, 9444−9450

alloy HNWAs, as manifested in SEM characterization (Figure S6). The XPS studies (Figure S7) also clearly demonstrate the presence of Pt and Ni signals in PtNi HNWAs. Furthermore, element mapping analysis of a single PtNi nanowire, which peeled from the PtNi HNWAs, is exhibited in Figure S8, which demonstrates the existence of Pt, Ni, Cd, and S elements in the as-prepared samples and their uniform distribution in the HNWAs. In electrochemical measurements, although both PtNi HNWAs and SNWAs exhibited a methanol oxidation peak at ca. +0.65 V, the peak current of PtNi alloy HNWAs was about 2 times higher than that of PtNi SNWAs, again, due to enhanced surface accessibility of the former. Figure S9 shows the typical voltammograms of PtNi HNWAs and SNWAs in a solution containing 0.5 M CH_3OH and 0.5 M H_2SO_4. For methanol oxidation reaction, it is widely known that the ratio of the forward anodic peak current (I_f) to the backward anodic peak current (I_b) can be used to evaluate the tolerance against carbonaceous poisoning species, where a low I_f/I_b value suggests incomplete oxidation of methanol to CO_2 during the forward anodic scan and residual carbonaceous species are accumulated on the Pt-catalyst surface. From Figure S9, the I_f/I_b ratio was found to be approximately 3.0 for the PtNi HNWAs (curve 1, Figure S9), considerably higher than that (1.4) of Pt HNWAs (curve 1, Figure 4b), suggesting much enhanced tolerance against CO poisoning by Ni alloying. The electrocatalytic stability of Pt HNWAs toward methanol oxidation reaction was investigated by a long-term current−time ($I-t$) measurement technique, as shown in Figure S10. As the electrodeposition time was increased from 60 to 3600 s, the as-synthesized Pt HNWAs show the high-steady current density for methanol oxidation reaction over the entire time range (3200 s), which indicates its superior durability. However, when the electrodeposition time was further increased to 7200 s, an obvious decrease of the voltammetric peak current was observed instead. Their differences in stability can probably be attributed to the different capabilities of the CO tolerance. As shown in Figure 4b, a notable difference in their I_f/I_b ratio was found from the samples prepared from 3600 s (1.38) and 7200 s (1.20) electrodeposition, respectively.

4. CONCLUSIONS

A simple, effective strategy was reported for the construction of Pt and PtNi hierarchical nanowire arrays at room temperature by an electrochemical deposition method, where CdS hierarchical nanowire arrays in AAO nanochannels were employed as a sacrificial template. In contrast with Pt solid nanowire arrays, Pt hierarchical nanowire arrays were composed of well-separated Pt NPs and exhibited larger electrochemical active surface areas. Significantly, the anodic peak current for methanol oxidation of Pt hierarchical nanowire arrays was almost 1 order of magnitude higher than that of Pt solid nanowire arrays. Furthermore, the formation of PtNi alloy hierarchical nanowire arrays resulted in reducing catalyst poisoning in the methanol electro-oxidation process. Such a synthetic method can potentially be extended as a universal approach to the preparation of hierarchical nanostructured catalysts with excellent performance.

ASSOCIATED CONTENT

Supporting Information

The Supporting Information is available free of charge on the ACS Publications website at DOI: 10.1021/acsami.7b19727.

SEM images, XRD spectra, XPS spectra, EDX spectra, element mapping analysis, and results of electrochemical measurements as noted in the text (PDF)

AUTHOR INFORMATION

Corresponding Authors

*E-mail: zhangyang@binn.cas.cn (Y.Z.).
*E-mail: qwchem@gmail.com (Q.W.).
*E-mail: lzfan@bnu.edu.cn (L.F.).
*E-mail: shaowei@ucsc.edu (S.C.).

ORCID

Changzheng Wang: 0000-0001-9111-6866
Yang Zhang: 0000-0002-3002-4367
Louzhen Fan: 0000-0003-0958-7015
Shaowei Chen: 0000-0002-3668-8551

Notes

The authors declare no competing financial interest.

ACKNOWLEDGMENTS

This work is financially supported by the National Natural Science Foundation of China (NSFC Nos. 21471103, 21603014, 51278026, 51578035, 21573019, 21233003, and 21103008).

REFERENCES

(1) Reddington, E.; Sapienza, A.; Gurau, B.; Viswanathan, R.; Sarangapani, S.; Smotkin, E. S.; Mallouk, T. E. Combinatorial Electrochemistry: A Highly Parallel, Optical Screening Method for Discovery of Better Electrocatalysts. *Science* **1998**, *280*, 1735−1737.
(2) Winter, M.; Brodd, R. J. What are Batteries, Fuel Cells, and Supercapacitors? *Chem. Rev.* **2004**, *104*, 4245−4269.
(3) Chen, C. Y.; Yang, P. Performance of an Air-breathing Direct Methanol Fuel Cell. *J. Power Sources* **2003**, *123*, 37−42.
(4) Arico, A. S.; Srinivasan, S.; Antonucci, V. DMFCs: From Fundamental Aspects to Technology Development. *Fuel Cells* **2001**, *1*, 133−161.
(5) Liang, Z.; Zhao, T. New DMFC Anode Structure Consisting of Platinum Nanowires Deposited into a Nafion Membrane. *J. Phys. Chem. C* **2007**, *111*, 8128−8134.
(6) Yang, S.; Zhao, C.; Ge, C.; Dong, X.; Liu, X.; Liu, Y.; Fang, Y.; Wang, H.; Li, Z. Ternary Pt-Ru-SnO_2 Hybrid Architectures: Unique Carbon-mediated 1-D Configuration and Their Electrocatalytic Activity to Methanol Oxidation. *J. Mater. Chem.* **2012**, *22*, 7104−7107.
(7) Liang, H.-P.; Zhang, H.; Hu, J.; Guo, Y.; Wan, L.; Bai, C. Pt Hollow Nanospheres: Facile Synthesis and Enhanced Electrocatalysts. *Angew. Chem., Int. Ed.* **2004**, *43*, 1540−1543.
(8) Zhao, Y.; Fan, L.; Zhong, H.; Li, Y.; Yang, S. Platinum Nanoparticle Clusters Immobilized on Multiwalled Carbon Nanotubes: Electrodeposition and Enhanced Electrocatalytic Activity for Methanol Oxidation. *Adv. Funct. Mater.* **2007**, *17*, 1537−1541.
(9) Tiwari, J. N.; Tiwari, R. N.; Singh, G.; Kim, K. S. Recent Progress in the Development of Anode and Cathode Catalysts for Direct Methanol Fuel Cells. *Nano Energy* **2013**, *2*, 553−578.
(10) Chen, C.; Kang, Y.; Huo, Z.; Zhu, Z.; Huang, W.; Xin, H. L.; Snyder, J. D.; Li, D.; Herron, J. A.; Mavrikakis, M.; Chi, M.; More, K. L.; Li, Y.; Markovic, N. M.; Somorjai, G. A.; Yang, P.; Stamenkovic, V. R. Highly Crystalline Multimetallic Nanoframes with Three-dimensional Electrocatalytic Surfaces. *Science* **2014**, *343*, 1339−1343.
(11) Xu, H.; Wang, A.; Tong, Y.; Li, G. Enhanced Catalytic Activity and Stability of Pt/CeO_2/PANI Hybrid Hollow Nanorod Arrays for Methanol Electro-oxidation. *ACS Catal.* **2016**, *6*, 5198−5206.
(12) Jiang, B.; Li, C.; Tang, J.; Takei, T.; Kim, J. H.; Ide, Y.; Henzie, J.; Tominaka, S.; Yamauchi, Y. Tunable-Sized Polymeric Micelles and Their Assembly for the Preparation of Large Mesoporous Platinum Nanoparticles. *Angew. Chem., Int. Ed.* **2016**, *55*, 10037−10041.

(13) Steele, B. C. H.; Heinzel, A. Materials for Fuel-cell Technologies. *Nature* **2001**, *414*, 345−352.
(14) Bell, A. T. The impact of Nanoscience on Heterogeneous Catalysis. *Science* **2003**, *299*, 1688−1691.
(15) Pu, L.; Zhang, H.; Yuan, T.; Zou, Z.; Zou, L.; Li, X.; Yang, H. High Performance Platinum Nanorod Assemblies based Double-layered Cathode for Passive Direct Methanol Fuel Cells. *J. Power Sources* **2015**, *276*, 95−101.
(16) Huang, H.; Yang, S.; Vajtai, R.; Wang, X.; Ajayan, P. M. Pt-Decorated 3D Architectures Built from Graphene and Graphitic Carbon Nitride Nanosheets as Efficient Methanol Oxidation Catalysts. *Adv. Mater.* **2014**, *26*, 5160−5165.
(17) Tian, N.; Zhou, Z.; Sun, S.; Ding, Y.; Wang, Z. L. Synthesis of Tetrahexahedral Platinum Nanocrystals with High-index Facets and High Electro-oxidation Activity. *Science* **2007**, *316*, 732−735.
(18) Ahmadi, T. S.; Wang, Z. L.; Green, T. C.; Henglein, A.; ElSayed, M. A. Shape-controlled Synthesis of Colloidal Platinum Nanoparticles. *Science* **1996**, *272*, 1924−1926.
(19) Zhang, J.; Yi, X.; Liu, S.; Fan, H.; Ju, W.; Wang, Q.; Ma, J. Vertically Aligned Carbon Nanotubes/Carbon Fiber Paper Composite to Support Pt Nanoparticles for Direct Methanol Fuel Cell Application. *J. Phys. Chem. Solids* **2017**, *102*, 99−104.
(20) Zhang, G.; Yang, Z.; Zhang, W.; Wang, Y. Nanosized Mo-doped CeO_2 Enhances the Electrocatalytic Properties of the Pt Anode Catalyst in Direct Methanol Fuel Cells. *J. Mater. Chem. A* **2017**, *5*, 1481−1487.
(21) He, C.-L.; Jiang, Y. X.; Rao, L.; Wang, Q.; Zhang, B. W.; Li, Y. Y.; Sun, S. G. Synthesis of Ultrafine Size Platinum Nanoparticles on Defective Graphene with Enhanced Performance Towards Methanol Electro-Oxidation. *Fuel Cells* **2013**, *13*, 873−880.
(22) Ding, L.-X.; Wang, A.; Li, G.; Liu, Z.; Zhao, W.; Su, C.; Tong, Y. Porous Pt-Ni-P Composite Nanotube Arrays: Highly Electroactive and Durable Catalysts for Methanol Electrooxidation. *J. Am. Chem. Soc.* **2012**, *134*, 5730−5733.
(23) Zhang, J.; Guo, S.; Wei, J.; Xu, Q.; Yan, W.; Fu, J.; Wang, S.; Cao, M.; Chen, Z. High-Efficiency Encapsulation of Pt Nanoparticles into the Channel of Carbon Nanotubes as an Enhanced Electrocatalyst for Methanol Oxidation. *Chem. - Eur. J.* **2013**, *19*, 16087−16092.
(24) Huang, M.; Zhang, J.; Wu, C.; Guan, L. Networks of Connected Pt Nanoparticles Supported on Carbon Nanotubes as Superior Catalysts for Methanol Electrooxidation. *J. Power Sources* **2017**, *342*, 273−278.
(25) Puthiyapura, V. K.; Brett, D. J. L.; Russell, A. E.; Lin, W.; Hardacre, C. Biobutanol as Fuel for Direct Alcohol Fuel Cells-Investigation of Sn-Modified Pt Catalyst for Butanol Electro-oxidation. *ACS Appl. Mater. Interfaces* **2016**, *8*, 12859−12870.
(26) Li, S.-S.; Zheng, J.; Ma, X.; Hu, Y.; Wang, A.; Chen, J.; Feng, J. Facile Synthesis of Hierarchical Dendritic PtPd Nanogarlands Supported on Reduced Graphene Oxide with Enhanced Electrocatalytic Properties. *Nanoscale* **2014**, *6*, 5708−5713.
(27) Zhang, L. M.; Wang, Z. B.; Zhang, J. J.; Sui, X. L.; Zhao, L.; Han, J. C. Investigation on Electrocatalytic Activity and Stability of Pt/C Catalyst Prepared by Facile Solvothermal Synthesis for Direct Methanol Fuel Cell. *Fuel Cells* **2015**, *15*, 619−627.
(28) Aboagye, A.; Elbohy, H.; Kelkar, A. D.; Qiao, Q.; Zai, J.; Qian, X.; Zhang, L. Electrospun Carbon Nanofibers with Surface-attached Platinum Nanoparticles as Cost-Effective and Efficient Counter Electrode for Dye-sensitized Solar Cells. *Nano Energy* **2015**, *11*, 550−556.
(29) Zhang, Q.; Cao, G. Hierarchically Structured Photoelectrodes for Dye-sensitized Solar Cells. *J. Mater. Chem.* **2011**, *21*, 6769−6774.
(30) Tian, J.; Uchaker, E.; Zhang, Q.; Cao, G. Hierarchically Structured ZnO Nanorods-Nanosheets for Improved Quantum-Dot-Sensitized Solar Cells. *ACS Appl. Mater. Interfaces* **2014**, *6*, 4466−4472.
(31) Wang, C.; E, Y.; Fan, L.; Wang, Z.; Liu, H.; Li, Y.; Yang, S.; Li, Y. Directed Assembly of Hierarchical CdS Nanotube Arrays from CdS Nanoparticles: Enhanced Solid State Electro-chemiluminescence in H_2O_2 Solution. *Adv. Mater.* **2007**, *19*, 3677−3681.
(32) Zhu, Y.; Ma, T.; Liu, Y.; Ren, T.; Yuan, Z. Metal Phosphonate Hybrid Materials: From Densely Layered to Hierarchically Nanoporous Structures. *Inorg. Chem. Front.* **2014**, *1*, 360−383.
(33) Wang, C.; E, Y.; Fan, L.; Yang, S.; Li, Y. CdS-Ag Nanocomposite Arrays: Enhanced Electro-chemiluminescence But Quenched Photoluminescence. *J. Mater. Chem.* **2009**, *19*, 3841−3846.
(34) Zhang, Y.; Jiang, L.; Li, H.; Fan, L.; Hu, W.; Wang, C.; Li, Y.; Yang, S. Single-Crystalline C_{60} Nanostructures by Sonophysical Preparation: Tuning Hollow Nanobowls as Catalyst Supports for Methanol Oxidation. *Chem. - Eur. J.* **2011**, *17*, 4921−4926.
(35) Zhang, X.; Wu, E.; Hu, D.; Bo, Z.; Zhu, W.; Yu, K.; Yu, C.; Wang, Z.; Yan, J.; Cen, K. Highly-branched Vertically-oriented Graphene Nanosheets with Dense Open Graphitic Edge Planes as Pt Support for Methanol Oxidation. *Phys. Status Solidi B* **2014**, *251*, 829−837.
(36) Mu, Y.; Liang, H.; Hu, J.; Jiang, L.; Wan, L. Controllable Pt Nanoparticle Deposition on Carbon Nanotubes as an Anode Catalyst for Direct Methanol Fuel Cells. *J. Phys. Chem. B* **2005**, *109*, 22212−22216.
(37) Radhakrishnan, T.; Sandhyarani, N. Three Dimensional Assembly of Electrocatalytic Platinum Nanostructures on Reduced Graphene Oxide - An Electrochemical Approach for High Performance Catalyst for Methanol Oxidation. *Int. J. Hydrogen Energy* **2017**, *42*, 7014−7022.
(38) Yamauchi, Y.; Tonegawa, A.; Komatsu, M.; Wang, H. J.; Wang, L.; Nemoto, Y.; Suzuki, N.; Kuroda, K. Electrochemical Synthesis of Mesoporous Pt-Au Binary Alloys with Tunable Compositions for Enhancement of Electrochemical Performance. *J. Am. Chem. Soc.* **2012**, *134*, 5100−5109.
(39) Yamauchi, Y.; Takai, A.; Nagaura, T.; Inoue, S.; Kuroda, K. Pt fibers with Stacked Donut-like Mesospace by Assembling Pt Nanoparticles: Guided Deposition in Physically Confined Self-Assembly of Surfactants. *J. Am. Chem. Soc.* **2008**, *130*, 5426−5427.
(40) Zhu, J.; He, G.; Shen, P. K. A Cobalt Phosphide on Carbon Decorated Pt Catalyst with Excellent Electrocatalytic Performance for Direct Methanol Oxidation. *J. Power Sources* **2015**, *275*, 279−283.
(41) Sun, Y.; Mayers, B.; Xia, Y. Metal Nanostructures with Hollow Interiors. *Adv. Mater.* **2003**, *15*, 641−646.
(42) Mostafa, E.; Abd-El-Latif, A. A.; Baltruschat, H. Electrocatalytic Oxidation and Adsorption Rate of Methanol at Pt Stepped Single-Crystal Electrodes and Effect of Ru Step Decoration: A DEMS Study. *ChemPhysChem* **2014**, *15*, 2029−2043.
(43) Chen, G.; Xia, D.; Nie, Z.; Wang, Z.; Wang, L.; Zhang, L.; Zhang, J. Facile Synthesis of Co-Pt Hollow Sphere Electrocatalyst. *Chem. Mater.* **2007**, *19*, 1840−1844.
(44) Maksimuk, S.; Yang, S.; Peng, Z.; Yang, H. Synthesis and Characterization of Ordered Intermetallic PtPb Nanorods. *J. Am. Chem. Soc.* **2007**, *129*, 8684−8685.
(45) Cao, X.; Wang, N.; Han, Y.; Gao, C.; Xu, Y.; Li, M.; Shao, Y. PtAg Bimetallic Nanowires: Facile Synthesis and Their Use as Excellent Electrocatalysts Toward Low-cost Fuel Cells. *Nano Energy* **2015**, *12*, 105−114.
(46) Gu, J.; Liu, W.; Zhao, Z.; Lan, G.; Zhu, W.; Zhang, Y. Pt/Ru/C Nanocomposites for Methanol Electrooxidation: How Ru Nanocrystals' Surface Structure Affects Catalytic Performance of Deposited Pt Particles. *Inorg. Chem. Front.* **2014**, *1*, 109−117.
(47) Chen, D.-J.; Tong, Y. J. Irrelevance of Carbon Monoxide Poisoning in the Methanol Oxidation Reaction on a PtRu Electrocatalyst. *Angew. Chem., Int. Ed.* **2015**, *54*, 9394−9398.
(48) Kadirgan, F.; Beyhan, S.; Atilan, T. Preparation and Characterization of Nano-sized Pt-Pd/C Catalysts and Comparison of Their Electro-activity Toward Methanol and Ethanol Oxidation. *Int. J. Hydrogen Energy* **2009**, *34*, 4312−4320.
(49) Kakati, N.; Maiti, J.; Lee, S. H.; Jee, S. H.; Viswanathan, B.; Yoon, Y. S. Anode Catalysts for Direct Methanol Fuel Cells in Acidic Media: Do We Have Any Alternative for Pt or Pt-Ru? *Chem. Rev.* **2014**, *114*, 12397−12429.
(50) Jiang, Q.; Jiang, L.; Hou, H.; Qi, J.; Wang, S.; Sun, G. Promoting Effect of Ni in PtNi Bimetallic Electrocatalysts for the Methanol

DOI: 10.1021/acsami.7b19727
ACS Appl. Mater. Interfaces 2018, 10, 9444−9450

Oxidation Reaction in Alkaline Media: Experimental and Density Functional Theory Studies. *J. Phys. Chem. C* **2010**, *114*, 19714−19722.
(51) Liao, Y.; Yu, G.; Zhang, Y.; Guo, T.; Chang, F.; Zhong, C. Composition-Tunable PtCu Alloy Nanowires and Electrocatalytic Synergy for Methanol Oxidation Reaction. *J. Phys. Chem. C* **2016**, *120*, 10476−10484.
(52) Samjeské, G.; Wang, H.; Loffler, T.; Baltruschat, H. CO and Methanol Oxidation at Pt-electrodes Modified by Mo. *Electrochim. Acta* **2002**, *47*, 3681−3692.
(53) Zhang, K.; Yang, W.; Ma, C.; Wang, Y.; Sun, C.; Chen, Y.; Duchesne, P.; Zhou, J.; Wang, J.; Hu, Y.; Banis, M.; Zhang, P.; Li, F.; Li, J.; Chen, L. A Highly Active, Stable and Synergistic Pt Nanoparticles/Mo_2C Nanotube Catalyst for Methanol Electro-oxidation. *NPG Asia Mater.* **2015**, *7*, No. e153.
(54) Yang, P.; Yuan, X.; Hu, H.; Liu, Y.; Zheng, H.; Yang, D.; Chen, L.; Cao, M.; Xu, Y.; Min, Y.; Li, Y.; Zhang, Q. Solvothermal Synthesis of Alloyed PtNi Colloidal Nanocrystal Clusters (CNCs) with Enhanced Catalytic Activity for Methanol Oxidation. *Adv. Funct. Mater.* **2018**, *28*, No. 1704774.
(55) Qiu, H. J.; Shen, X.; Wang, J. Q.; Hirata, A.; Fujita, T.; Wang, Y.; Chen, M. W. Aligned Nanoporous Pt-Cu Bimetallic Microwires with High Catalytic Activity toward Methanol Electrooxidation. *ACS Catal.* **2015**, *5*, 3779−3785.
(56) Elbaum, R.; Vega, S.; Hodes, G. Preparation and Surface Structure of Nanocrystalline Cadmium Sulfide (sulfoselenide) Precipitated from Dimethyl Sulfoxide Solutions. *Chem. Mater.* **2001**, *13*, 2272−2280.
(57) Sun, S.; Yang, D.; Villers, D.; Zhang, G.; Sacher, E.; Dodelet, J. Template- and Surfactant-free Room Temperature Synthesis of Self-assembled 3D Pt Nanoflowers from Single-crystal Nanowires. *Adv. Mater.* **2008**, *20*, 571−574.
(58) Do, I.; Drzal, L. T. Ionic Liquid-Assisted Synthesis of Pt Nanoparticles onto Exfoliated Graphite Nanoplatelets for Fuel Cells. *ACS Appl. Mater. Interfaces* **2014**, *6*, 12126−12136.
(59) Li, T.; You, H.; Xu, M.; Song, X.; Fang, J. Electrocatalytic Properties of Hollow Coral-like Platinum Mesocrystals. *ACS Appl. Mater. Interfaces* **2012**, *4*, 6942−6948.
(60) Xu, Y.; Lin, X. Selectively Attaching Pt-nano-clusters to the Open Ends and Defect Sites on Carbon Nanotubes for Electrochemical Catalysis. *Electrochim. Acta* **2007**, *52*, 5140−5149.
(61) Zheng, S.; Hu, J.; Zhong, L.; Wan, L.; Song, W. In Situ One-step Method for Preparing Carbon Nanotubes and Pt Composite Catalysts and Their Performance for Methanol Oxidation. *J. Phys. Chem. C* **2007**, *111*, 11174−11179.
(62) Antolini, E. Formation of Carbon-supported PtM Alloys for Low Temperature Fuel Cells: A Review. *Mater. Chem. Phys.* **2003**, *78*, 563−573.
(63) Reddy, A. L. M.; Ramaprabhu, S. Pt/SWNT-Pt/C Nanocomposite Electrocatalysts for Proton-exchange Membrane Fuel Cells. *J. Phys. Chem. C* **2007**, *111*, 16138−16146.

DOI: 10.1021/acsami.7b19727
ACS Appl. Mater. Interfaces 2018, 10, 9444−9450